BJP British Journal of Pharmacology

DOI:10.1111/bph.12572
www.brjpharmacol.org

RESEARCH PAPER

Reversal of SIN-1-induced eNOS dysfunction by the spin trap, DMPO, in bovine aortic endothelial cells via eNOS phosphorylation

Amlan Das[1§], Bhavani Gopalakrishnan[1§], Lawrence J Druhan[2], Tse-Yao Wang[1], Francesco De Pascali[1], Antal Rockenbauer[3], Ira Racoma[1], Saradhadevi Varadharaj[1], Jay L Zweier[1,4], Arturo J Cardounel[2] and Frederick A Villamena[1,5]

[1]*Davis Heart and Lung Research Institute, College of Medicine,* [2]*Department of Anesthesiology,* [4]*Department of Internal Medicine,* [5]*Department of Pharmacology, College of Medicine, The Ohio State University, Columbus, OH, USA, and* [3]*Institute of Molecular Pharmacology, Research Centre for Natural Sciences, Hungarian Academy of Sciences, Budapest, Hungary*

Correspondence
Frederick A Villamena, Davis Heart and Lung Research Institute, Department of Pharmacology, College of Medicine, The Ohio State University, 473 W. 12th Ave., Columbus, OH 43210, USA.
E-mail: villamena.1@osu.edu

[§]Both authors equally contributed to this work.

Keywords
eNOS; DMPO; spin trapping; endothelial dysfunction; peroxynitrite; oxidative stress; reactive oxygen species; nitric oxide; cardiovascular diseases; endothelial cells

Received
3 July 2013
Revised
3 December 2013
Accepted
18 December 2013

BACKGROUND AND PURPOSE

Nitric oxide (NO) derived from eNOS is mostly responsible for the maintenance of vascular homeostasis and its decreased bioavailability is characteristic of reactive oxygen species (ROS)-induced endothelial dysfunction (ED). Because 5,5-dimethyl-1-pyrroline-*N*-oxide (DMPO), a commonly used spin trap, can control intracellular nitroso-redox balance by scavenging ROS and donating NO, it was employed as a cardioprotective agent against ED but the mechanism of its protection is still not clear. This study elucidated the mechanism of protection by DMPO against SIN-1-induced oxidative injury to bovine aortic endothelial cells (BAEC).

EXPERIMENTAL APPROACH

BAEC were treated with SIN-1, as a source of peroxynitrite anion ($ONOO^-$), and then incubated with DMPO. Cytotoxicity following SIN-1 alone and cytoprotection by adding DMPO was assessed by MTT assay. Levels of ROS and NO generation from HEK293 cells transfected with wild-type and mutant eNOS cDNAs, tetrahydrobiopterin bioavailability, eNOS activity, eNOS and Akt kinase phosphorylation were measured.

KEY RESULTS

Post-treatment of cells with DMPO attenuated SIN-1-mediated cytotoxicity and ROS generation, restoration of NO levels via increased in eNOS activity and phospho-eNOS levels. Treatment with DMPO alone significantly increased NO levels and induced phosphorylation of eNOS Ser^{1179} via Akt kinase. Transfection studies with wild-type and mutant human eNOS confirmed the dual role of eNOS as a producer of superoxide anion (O_2^-) with SIN-1 treatment, and a producer of NO in the presence of DMPO.

CONCLUSION AND IMPLICATIONS

Post-treatment with DMPO of oxidatively challenged cells reversed eNOS dysfunction and could have pharmacological implications in the treatment of cardiovascular diseases.

Abbreviations

ACN, acetonitrile; BAEC, bovine aortic endothelial cells; BH_4, tetrahydrobiopterin; CM-H_2DCFDA, 5-(and-6)-chloromethyl-2′,7′-dichlorodihydrofluorescein diacetate, acetyl ester; DCFH-DA, 2,7-dichlorodihydrofluorescein diacetate; DHE, dihydroethidium; DMPO, 5,5-dimethyl-1-pyrroline-*N*-oxide; DTPA, diethylenetriamine pentaacetic acid; EMPO, 5-ethoxycarbonyl-5-methyl-1-pyrroline-*N*-oxide; hfsc, hyperfine splitting constant; Me-β-CD, methyl-β-cyclodextrin; METC: mitochondrial electron transport chain; MGD, N-methyl-D-glucamine dithiocarbamate; NXY-059, disodium-[(*tert*-butylimino) methyl] benzene-1,3-disulfonate *N*-oxide; PBN, α-phenyl-*N*-*tert*-butylnitrone; SIN-1, 3-morpholinosydnonimine

Introduction

Oxidative stress resulting from the overproduction of reactive oxygen species (ROS), leads to endothelial dysfunction which is implicated in the pathophysiology of several cardiovascular disorders such as atherosclerosis, hypercholesterolaemia, hypertension, type 2 diabetes and heart failure (Cai and Harrison, 2000; Heitzer *et al.*, 2001; Vita, 2011). Excessive ROS generation within the vasculature may lead to the oxidation of low-density lipoproteins, decreased bioavailability of endothelium-derived NO (O'Donnell and Freeman, 2001) and formation of peroxynitrite ($ONOO^-$), a highly reactive anion (Beckman and Koppenol, 1996). All these events contribute to the impaired function of the vascular endothelium.

Endothelium-derived NO is an important signalling molecule which regulates vessel homeostasis by inducing vascular smooth muscle relaxation, and inhibiting vascular smooth muscle hypertrophy, regulating platelet aggregation and leukocyte adhesion (Gross and Wolin, 1995). In the endothelium, NO is produced by a family of enzymes termed NO synthases (NOS; nomenclature follows Alexander *et al.*, 2013) that catalyze the conversion of L-arginine to L-citrulline and NO. The reactive oxygen and nitrogen species generated during oxidative stress are known to induce eNOS dysfunction that leads to the uncoupling of the enzyme and results in the production of NOS-derived $O_2^{\bullet-}$ instead of NO (Wei *et al.*, 2003). The resulting imbalance between NO and $O_2^{\bullet-}$ can contribute to the onset of a variety of cardiovascular diseases.

NOS activity is regulated by a complex cascade of phosphorylation/dephosphorylation at particular regulatory residues in the enzyme. Phosphorylation of eNOS Ser^{635} and Ser^{1179} leads to the activation of eNOS function while phosphorylation at Thr^{497} down-regulates it (Harris *et al.*, 2001; Michell *et al.*, 2001). Activation by eNOS Ser^{1179} phosphorylation results from the enhanced electron flux through the reductase domain and inhibition of calmodulin-dissociation from the enzyme in a calcium-independent fashion (Fulton *et al.*, 1999; McCabe *et al.*, 2000) and is mediated by several upstream kinases, among which PI3/Akt has been reported to play a crucial role in the regulation of enzyme activity (Fulton *et al.*, 1999).

Most of the NO donor drugs are limited only by their NO delivering property and usually exhibit uncontrolled delivery of NO because of their instability in blood plasma (Wang *et al.*, 2005). Nitrones can both scavenge reactive species (Villamena and Zweier, 2004; Villamena *et al.*, 2005) and also exhibit controlled release of NO as a consequence (Locigno *et al.*, 2005; Nash *et al.*, 2012), and are therefore, more desirable and different from current drugs. To date, there are two major types of nitrones: the cyclic nitrones which include 5,5-dimethyl-1-pyrroline-*N*-oxide (DMPO), 5-carbamoyl-5-methyl-1-pyrroline-*N*-oxide, 5-ethoxycarbonyl-5-methyl-1-pyrroline-*N*-oxide (EMPO), 5-(diethoxyphosphoryl)-5-methyl-1-pyrroline-*N*-oxide and the linear nitrones α-phenyl-*N*-*tert*-butylnitrone (PBN), (disodium-[(*tert*-butylimino) methyl] benzene-1,3-disulfonate *N*-oxide (NXY-059) which have been used to detect free radicals (Figure 1). Nitrones are structurally simple molecules, yet they possess rich chemistries and biological properties that make them important pharmacological agents (Zuo *et al.*, 2009; Das *et al.*, 2012; Traynham *et al.*, 2012; Villamena *et al.*, 2012; Zamora and Villamena, 2013). Nitrone spin traps such as DMPO, PBN and its derivative, NXY-059 have shown pharmacological activity against ischaemia and reperfusion (I/R) injury in the heart and brain (Floyd, 2009; Zuo *et al.*, 2009), neurodegeneration (Floyd *et al.*, 2013) and cancer (Floyd *et al.*, 2008; Floyd, 2009). NXY-059 was the first neuroprotective agent that reached a clinical trial phase in the USA (Floyd *et al.*, 2008). Application of DMPO as a cardioprotective agent was previously reported (Tosaki *et al.*, 1990) but its modes of action were unclear. DMPO also conferred protection against cardiac I/R injury in Langendorff rat heart preparations by salvaging the mitochondrial electron transport chain (METC) complexes and decreased ROS production (Zuo *et al.*, 2009). Other experimental evidence suggests involvement of other mechanisms for cardioprotection by DMPO other than its direct spin trapping properties, such as induction of phase II enzymes via nuclear translocation of the transcription factor NRF-2 and suppression of mitochondria-dependent proapoptotic signalling in endothelial cells (Das *et al.*, 2012). Increase in myocyte contraction via regulation of nitroso-redox levels and increase in sarcoplasmic reticulum Ca^{2+} handling have also been proposed (Traynham *et al.*, 2012).

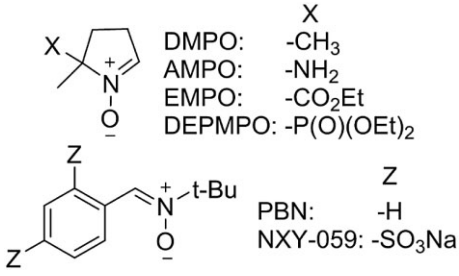

Figure 1
Chemical structures of various cyclic (above) and linear (below) nitrones.

Although the reversal of eNOS uncoupling via supplementation with tetrahydrobiopterin (BH_4) has already been described (Forstermann, 2006), in the present study, we explored the mechanism of reversal of eNOS dysfunction by post-treatment of endothelial cells with DMPO, after treating the cells with the peroxynitrite donor, 3-morpholinosydnonimine (SIN-1), offering another mechanistic insight into the cardioprotective property of nitrones.

Methods

Cell culture and maintenance

Bovine aortic endothelial cells (BAEC; Cell Systems, Kirkland, WA) were cultured using a T75 cm^2 flask in DMEM medium with 1 g L^{-1} D-glucose and 4 mM L-glutamine, and supplemented with 10% FBS, 50 μg mL^{-1} pencillin, 50 μg mL^{-1} streptomycin, 2.5 mg L^{-1} endothelial cell growth supplement and 1% MEM-non-essential amino acids at 37°C in a humidified atmosphere of 5% CO_2 and 20% O_2. HEK293 were cultured under same conditions in DMEM media without endothelial cell growth supplement and MEM-non-essential amino acids. The medium was changed every 2–3 days and cells were subcultured once they reached 90–95% confluence or 80% for HEK293 cells.

SIN-1 and DMPO treatment of cells

BAEC or HEK293 cells were seeded at a density of 10^4 cells mL^{-1} in each well using a 24-well plate and grown to 70% confluency. Cells were treated with 500 μM SIN-1 for 2 h, and then post-incubated in plain medium without SIN-1 for additional 24 h, in the absence or presence of DMPO. Cell viability was assessed by MTT assay following the protocol described previously (Das *et al.*, 2010). Cell viability was calculated as the percentage of inhibition by the following formula (Equation 1):

$$\%\ \text{inhibition} = [1 - A_t/A_s] \times 100\% \quad (1)$$

where A_t and A_s are absorbance of the sample and solvent alone respectively. Results were presented as mean ± SEM, where $n = 6$.

ROS detection by confocal microscopy

Cells with density of 10^4 cells mL^{-1} were seeded on sterile glass cover slips 6-well plate. Treated cells were fixed with 10% paraformaldehyde at room temperature for 10 min, washed with PBS three times and subsequently incubated with 25 μM of the fluorogenic probe 2,7-dichlorodihydrofluorescein diacetate (DCFH-DA) or 10 μM dihydroethidium (DHE) for 30 min at 37°C, followed by nuclei staining with DAPI (1 μM) for 30 min. Images were then captured by Olympus FluoView-1000 confocal microscope (Olympus, Shinjuku, Tokyo, Japan) using an excitation/emission filter of 543/602 nm for DHE, 488/535 nm for DCFH-DA and 405/422 nm for DAPI. Fluorescence intensities of 100 cells from different fields were calculated and results were presented as mean ± SEM of three independent experiments ($n = 3$).

ROS and NO detection by EPR spin trapping

Cells (10^4 cells mL^{-1}) were grown to 70% confluency in 6-well plates. After SIN-1 treatment, cells were incubated with 150 μL of EMPO (25 mM) and 150 μL of methyl-β-cyclodextrin (Me-β-CD; 50 mM) and 10 μL of 10 μM CaI for 15 min (Šnyrychová, 2010). The supernatant (300 μL) was transferred to a quartz flat cell and spin adduct formation was detected at room temperature using Bruker EMX X-Band EPR spectrometer (Bruker Corp., Billerica, MA, USA). Experiment was repeated in the presence or absence of DMPO post-incubation. Instrument parameters were as follows: microwave frequency, 9.8 GHz; centre field, 3485 G; modulation amplitude, 0.2–1.0 G; microwave power, 10 mW; conversion time: 41 ms; time constant: 82 ms, sweep time: 42 s; sweep width: 120 G; receiver gain, 1×10^5 and using incremental sweep. Spectra were simulated using an automatic fitting programme (Rockenbauer and Korecz, 1996) where the pertinent hyperfine splitting constants of $HO_2^{\bullet}$, $HO^{\bullet}$ and C-centred adducts and their concentrations from the total area of each spectrum were obtained. Adducts were independently prepared using hypoxanthine-xanthine oxidase, Fe^{2+}-H_2O_2 and Fe^{2+}-H_2O_2-ethanol for $HO_2^{\bullet}$, $HO^{\bullet}$ and C-centred adducts respectively (Supporting Information Table S3). Spectra were obtained from three independent experiments ($n = 3$). Using the same cell cultures in 6-well plates, generation of NO in cells were detected by EPR spin trapping using the ferrous N-methyl-D-glucamine dithiocarbamate complex ($Fe(MGD)_2$) as the spin trap following the published protocol (Gopalakrishnan *et al.*, 2012). Cells were washed with PBS after treatment, then incubated for 15 min with PBS with $CaCl_2$ and $MgCl_2$, calcium ionophore A21387 (10 μM), $FeSO_4$ (3.5 mM) and NH_4MGD (20.8 mM; Shinobu *et al.*, 1984) at a final volume of 500 μL. The supernatant (300 μL) was transferred to a quartz flat cell and spin adduct formation was detected at room temperature with EPR instrument parameters: microwave frequency, 9.8 GHz; centre field, 3426.5 G; modulation amplitude, 6 G; microwave power, 12 mW; conversion time: 10 ms; time constant: 20 ms, sweep time: 10 s; sweep width: 100 G; receiver gain, 1×10^5 and using incremental sweep. The two-dimensional spectra were integrated and baseline corrected using Bruker WinEPR data processing software (Bruker Corp.). Results are as mean ± SEM of three independent experiments ($n = 3$).

BAEC in a T75 cm^2 culture flask were serum-starved overnight then endogenous L-[^{14}N]-arginine was exchanged for L-[^{15}N]-arginine by incubating cells with Tyrode's solution supplemented with 84 mg L^{-1} L-[^{15}N]-arginine (98 atom% [^{15}N], Isotec Sigma-Aldrich, St. Louis, MO) for 30 min at 37°C. After incubation, cells were washed with PBS, treated with $Fe(MGD)_2$ as above and EPR spectra were acquired (Gopalakrishnan *et al.*, 2012).

Determination of eNOS activity

eNOS activity was determined using the conversion of arginine to citrulline assay with [^{14}C]arginine (12.1 GBq/mmol; Moravek Biochemicals, Brea, CA) as a substrate using the previously published protocol with a slight modification (Giraldez and Zweier, 1998). Cultured BAEC (10^4 cells mL^{-1}) were grown to 70% confluency in T75 cm^2 culture flask and subjected to SIN-1 treatment and DMPO post-treatment. After treatment, eNOS activity was measured by L-[^{14}C]arginine to L-[^{14}C]citrulline conversion in a total volume of 50 μL buffer containing 50 mM Tris-HCl, pH 7.4, 1 μM L-[^{14}C]arginine (605 Bq per incubation sample), 1 mM

NADPH, 0.6 mM Ca^{2+}, 2.5 μM calmodulin and 10 μM BH_4. After 10 min incubation at 37°C, the mixture was terminated by adding 400 μL of stop buffer (20 mM HEPES, pH 5.5, 2 mM EDTA, 2 mM EGTA). L-[^{14}C]citrulline was separated by mixing the reaction mixtures with 100 μL of pre-equilibrated Dowex AG 50W-X8 (Na^+ form) cation exchange resin (Bio-Rad Laboratories, Hercules, CA, USA), then passed through spin columns and quantitated by liquid scintillation counter. Results were presented as mean ± SEM of three independent experiments (n = 3).

Measurement of BH_4 by HPLC

The total BH_4 content was measured using HPLC analysis as described elsewhere (Hyland, 1985; Dumitrescu *et al.*, 2007). Cells were grown in T75 cm^2 flask up to 70% confluency. SIN-1-treated cells were washed once with PBS and lysed with lysis buffer containing 1 mM ascorbate, 1 mM DTT and 100 μM diethylenetriamine pentaacetic acid (DTPA), followed by sonication. The mixture was then centrifuged at 12,000 × g for 1 min at 4°C. The supernatant containing the protein was removed by filtration through a Microcom YM-3 spin column (Millipore Corp. Billerica, MA, USA). The filtrates were injected into an ESA HPLC system with a C-18 column (T3 4.6 × 150 mm 5 micron) and HPLC separation was performed as described earlier (Hyland, 1985; Dumitrescu *et al.*, 2007) using a mobile phase comprising 50 mM potassium phosphate, 10 mM phosphate monobase, 12% acetonitrile, 6 mM citric acid, 1 mM DTT, 5 mM octyl sulfate, pH 3 and isocratic elution at 1.2 mL min^{-1}. Detection parameters were: 35 and 500mV for electrochemical cell; fluorescence: excitation at 348 nm and emission at 444 nm; UV at 254 nm. Results were expressed as means ± SEM of three independent experiments (n = 3).

Western blot analysis

Western blot analysis was performed to determine the expression levels of p-eNOS, p-Akt, total (t)-Akt and t-eNOS proteins in untreated, SIN-1-treated and nitrone-post-incubated SIN-1-treated BAEC. Prior to treatment, cultured BAEC (10^4 cells mL^{-1}) were grown to 70% confluency on 60 mm Petri-dishes, and 50 μg of protein from each set was used for Western blotting. In a separate experimental set, the membrane was incubated with rabbit polyclonal anti-p-eNOS (Ser^{1179}) Ab (1:1000 dilution, Cell Signaling Technology, Danvers, MA, USA), mouse monoclonal anti-p-Akt (Ser^{473}) Ab (1:500 dilution, Cell Signaling Technology), mouse monoclonal anti-t-eNOS Ab (1:1000 dilution, Santa Cruz Biotechnology, Paso Robles, CA, USA), rabbit polyclonal anti-t-Akt Ab (1:500 dilution, Cell Signaling Technology) and mouse monoclonal anti-β-actin Ab (1:1000 dilution, Santa Cruz Biotechnology) overnight at 4°C. The protein bands were visualized using a chemiluminiscence kit (Thermo Scientific, Waltham, MA, USA), and the bands were quantified densitometrically by Bio-Rad Chemi Doc (1708070) system using the software Quantity One (Bio-Rad).

Transient transfection of HEK293 cells with wild-type and mutant eNOS cDNAs

HEK cells were transfected with 5 μg μL of eNOS cDNA (wild-type and mutant where Ser^{1179} was changed to alanine) (Lin *et al.*, 2003) using Lipofectamine™ 2000 (Invitrogen, Carlsbad, CA, USA) according to the manufacturer's instructions. The transfection efficiency was analysed using Western blot analysis of eNOS proteins and by measuring NO levels.

Data analysis

Data are presented as the mean (±SEM) of at least three independent experiments. Data were analysed by one-way ANOVA, with the Student-Newman-Keul *post hoc* test, using Sigma plot 12.0 (Systat Software, Inc, San Jose, CA, USA). P values <0.05 were considered to be statistically significant.

Materials

The reagents used were supplied as follows: 5-(and-6)-chloromethyl-2′,7′-dichlorodihydrofluorescein diacetate, acetyl ester (CM-H_2DCFDA) by Invitrogen (Eugene, OR, USA); DAPI, DCFH-DA, DTPA, Me-β-CD by Sigma; DHE by Molecular Probes (Eugene, OR, USA); DMPO by Dojindo (Rockville, MD, USA); SIN-1 by Enzo Life Science (Farmingdale, NY, USA).

Results

Dose- and time-dependent cytoprotective effects from post-treatment by DMPO of SIN-1-challenged BAEC

Treatment of cells with varying concentrations of DMPO alone (25–500 μM) for 24 h did not result in loss of cell viability (Supporting Information Figure S1). However, cells challenged with 500 μM SIN-1, over a range of times, resulted in significant cytotoxicity (Supporting Information Figure S2). For instance, a 50% decrease in cell viability was observed after 2 h of SIN-1 treatment followed by 24 h of post-incubation in plain media (without SIN-1) (Supporting Information Figure S2). SIN-1 has been suggested to induce cell death via two mechanisms, production of $ONOO^-$ through reaction between NO and $O_2^{\bullet-}$ to finally form $HO^\bullet$ (Ishii *et al.*, 1999), and generation of H_2O_2 (Lomonosova *et al.*, 1998). When SIN-1-challenged cells were post-incubated with DMPO, cell viability was increased, in both dose- and time-dependent fashion (Figures 2A and B). The greatest cytoprotection was obtained when SIN-1-treated cells were post-incubated with 100 μM of DMPO for 24 h, compared with pretreatment of BAEC with DMPO for 24 h before 2 h SIN-1 treatment, a procedure that did not significantly change cell viability (data not shown). We therefore used post-treatment with 100 μM of DMPO after SIN-1 challenge, in all subsequent experiments.

Attenuation of ROS generation in SIN-1-treated BAEC by DMPO

To test if the cells generated O_2^- after treatment with SIN-1, EPR spin trapping was performed using EMPO/Me-β–CD as spin trap on SIN-1-treated BAEC at various times (0–24 h) of incubation. EPR results showed increased ROS intensities with increasing time of post-incubation along with the formation of a C-centred adduct which could be formed as a secondary product (Supporting Information Figure S3A and Table S1 for the simulation). The low-field peak intensity of

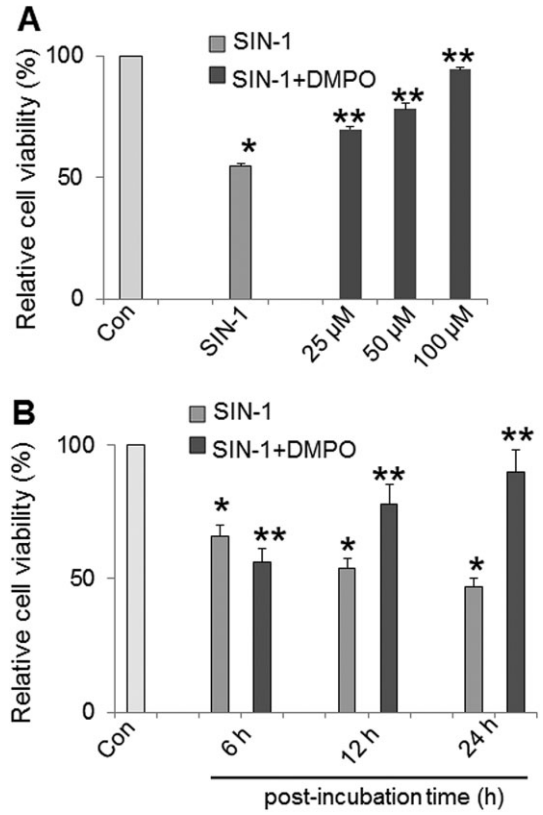

Figure 2

Effect of DMPO on SIN-1-induced cytotoxicity. (A) Dose-dependence, (B) Time-dependence. Cell viability was measured using the MTT assay. All data are means ± SEM, *<0.05 versus control (untreated cells), **<0.05 versus SIN-1-treated cells; one-way ANOVA, Tukey's test, $n = 6$.

the EPR spectra increased significantly in SIN-1-treated cells by up to 2.9-fold after 24 h of post-incubation (Supporting Information Figure S3B). EPR results were confirmed by confocal microscopy using DHE staining of SIN-1-treated cells at different time points. Treatment of cells with SIN-1 for 2 h (corresponding to 0 h of post-incubation) resulted in a significant increase of DHE-fluorescence specific for O_2^- and the signal persisted for up to 6 h of post-incubation in plain media, with fluorescence decreases upon further incubation for 12 and 24 h (Supporting Information Figure S4).

As H_2O_2 could be also formed from SIN-1 treatment via O_2^- dismutation (Lomonosova *et al.*, 1998), we performed a time-dependent confocal microscopy study on SIN-1-treated BAEC by staining the cells with the ROS-specific fluorescent probe, CM-H_2DCFDA (Figure S5). SIN-1-untreated BAEC showed no detectable DCF-fluorescence signal indicating that the cells did not produce $O_2^{\bullet-}$-derived ROS. However, when BAEC were treated with SIN-1 for 2 h and incubated without SIN-1 for an additional 24 h, a time-dependent accumulation of DCF-fluorescence signal was detected (Supporting Information Figure S5).

When SIN-1-challenged cells were post-treated with 100 μM DMPO, DCF-fluorescence intensity was significantly decreased (Figures 3A and B) compared to a threefold increase in DCF-fluorescence in SIN-1-treated cells without DMPO post-treatment. Simulation of the EPR spectra also revealed that the concentration of O-centred adduct was significantly decreased with a concomitant decrease in the concentration of C-centred adducts when SIN-1-treated BAEC were post-incubated with DMPO for 24 h (Supporting Information Table S2 and Figures 3C and D).

Restoration of NO bioavailability in SIN-1-treated BAEC by DMPO

As oxidative stress leads to decreased bioavailability of NO (Cai and Harrison, 2000), the effect of SIN-1 on NO production in BAEC was investigated. Using EPR and $Fe(MGD)_2$ as spin trap to detect NO generation (Figures 4A and B), a significant decrease in NO production of almost 50% was observed when cells were treated with SIN-1 for 2 h and post-incubated in plain media for 24 h. The same observation was previously reported for BAEC upon treatment with SIN-1 or $ONOO^-$ (Kuzkaya *et al.*, 2003). However, post-treatment with DMPO for 24 h resulted in the restoration of the NO levels by about 35%. Treatment of cells with the NOS inhibitor L-NAME, completely abolished the NO signal (Figure 4B), indicating that the NO was derived from enzymic activity of NOS.

Restoration of eNOS activity in SIN-1-treated BAEC by DMPO

eNOS activity was assessed using the L-[^{14}C] arginine to L-[^{14}C] citrulline conversion assay. BAEC were treated with SIN-1 for 2 h and post-incubated for another 24 h that resulted in significant inhibition of eNOS activity by ~30%. However, post-treatment with DMPO for 24 h led to the complete restoration of eNOS activity (Figure 4C). This provides definitive evidence that the effects of DMPO on NO production are mediated at least in part through increased eNOS-derived NO production and not merely a consequence of scavenging SIN-1-derived superoxide.

Increased bioavailability of NO in BAEC treated with DMPO alone

As post-treatment with DMPO resulted in a significant increase in NO production and NOS activity in SIN-challenged cells, we investigated if the nitrone alone could increase NO generation in BAEC, without oxidatively challenging the cells. EPR studies revealed that treatment of cells with DMPO alone resulted in a time-dependent increase in cellular NO and a 40% increase in NO production was observed after 24 h of treatment (Figure 5).

Determination of NO source: nitrone versus L-arginine

To determine if the source of the generated NO was from chemical decomposition of the nitrone (Locigno *et al.*, 2005) or from eNOS-catalyzed conversion of L-arginine to L-citrulline, an isotope-labelling experiment using L-[^{15}N]-arginine was carried out. Because of the difference in the nuclear spins of ^{14}N ($I = ½$) and ^{15}N ($I = 1$), it is possible to determine the source of NO formed (Xia and Zweier, 1997). A time-dependent formation of a doublet signal, characteristic

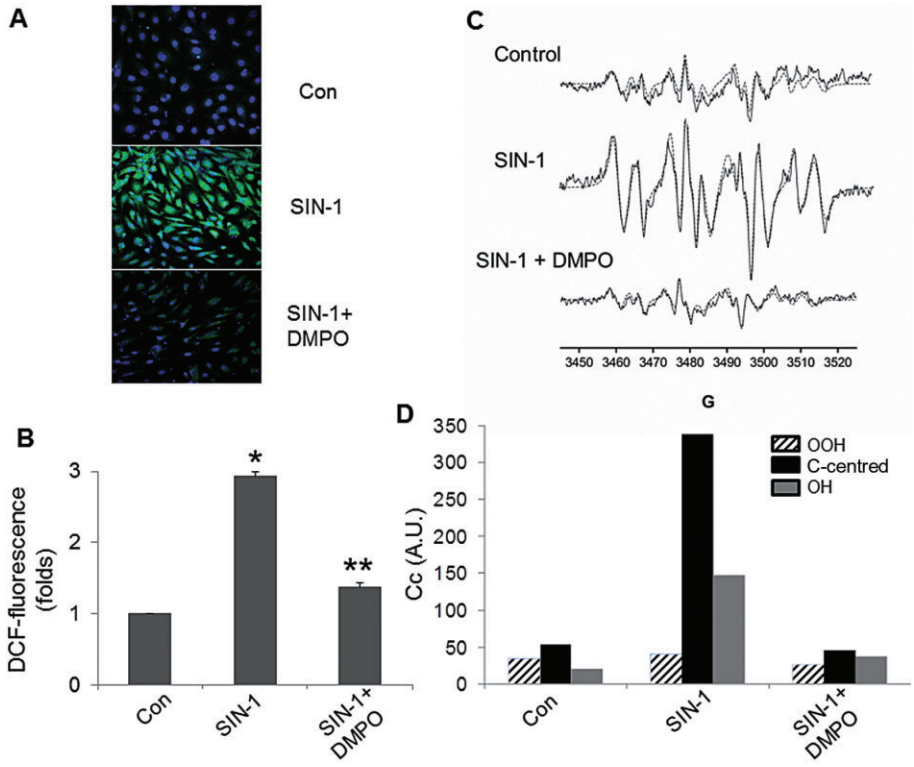

Figure 3

Effect of DMPO on SIN-1-induced ROS generation in BAEC. (A) Confocal micrographs of ROS generation in BAEC treated with SIN-1 (500 μM) alone and those post-incubated with DMPO (100 μM). (B) Plot of average DCF-fluorescence obtained from 100 cells. All data are means ± SEM, *$P < 0.05$ versus control (untreated cells), **$P < 0.05$ versus SIN-1-treated cells; one-way ANOVA, Tukey's test, $n = 3$. (C) Representative X-band EPR spectra and simulated (dotted lines) of radical adducts formed in SIN-1-treated BAEC, with and without DMPO (100 μM) incubation using EMPO/Me-β–CD as spin trap (see Supporting Information Table S2 for complete simulated EPR parameters). (D) Plot of the concentrations of the HO_2•, HO• and C-centred adducts from Figures 2C.

of ^{15}NO–Fe–MGD spectrum was observed (Figure 6A) after incubation of L-[^{14}N]-arginine-depleted BAEC with L-[^{15}N]-arginine for 24 h. Incubation of cells in the presence of DMPO and L-[^{15}N]-arginine for 24 h gave a similar doublet spectrum demonstrating that most of the detected NO were generated from the ^{15}N-labelled arginine (Figure 6B). This result suggests that the NO generated in BAEC upon DMPO treatment did not originate from the nitrone itself, but rather from the metabolism of L-arginine to L-citrulline, and thus, implied that NOS was the source of the NO.

Induction of eNOS- and Akt phosphorylation in BAEC by DMPO in the absence of SIN-1 treatment

Western blots were carried out to detect p-eNOS Ser^{1179} in BAEC treated with DMPO for 12 and 24 h. Levels of p-eNOS increased time-dependently after DMPO treatment, with a significant 2.2-fold increase after 12 h of incubation. The p-eNOS level was only slightly increased after 24 h of treatment (Figures 7A and B). As PKB or Akt is known to be an upstream regulator of eNOS and results in the phosphorylation of the enzyme (Fulton *et al.*, 1999), p-Akt Ser^{473} levels were also measured in the presence of DMPO. DMPO treatment of cells resulted in a similar time-dependent increase in p-Akt levels. Incubation of cells with DMPO for 12 and 24 h resulted in 2.7- and 3.5-fold increases in p-Akt levels respectively (Figures 7A and C). Therefore, these observations showed that DMPO could increase NO bioavailability in un-challenged BAEC via phosphorylation of Akt and eNOS.

Inhibition of SIN-1 mediated down-regulation of p-eNOS and p-Akt in BAEC by DMPO

The phosphorylation levels of eNOS increased by 22% after 2 h of SIN-1 treatment (corresponding to 0 h of post-incubation with DMPO) but there was a time-dependent decrease in p-eNOS levels during further incubation of SIN-1-treated cells in plain media. After 24 h of post-incubation, the p-eNOS band intensity decreased by 55% compared with control cells (Figures 8A and B). However, when SIN-1-challenged cells were post-treated with DMPO for 24 h, p-eNOS levels were significantly restored (Figures 8C and D). In addition, we also observed significant restoration of p-Akt levels in SIN-1-treated BAEC upon post-treatment with DMPO (Figures 8C and E). These observations show that DMPO can increase NO bioavailability in SIN-1-challenged BAEC, via phosphorylation of Akt and eNOS.

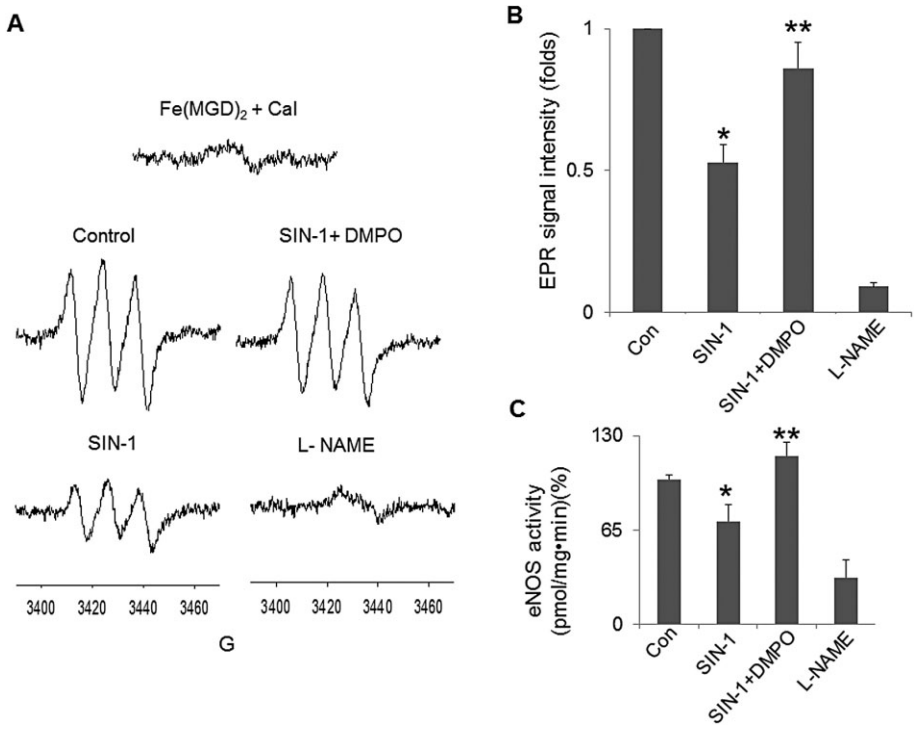

Figure 4

Restoration of NO production and eNOS activity in SIN-1-treated BAEC by DMPO. (A) X-band EPR spectra of NO using $Fe(MGD)_2$ spin trap, generated from SIN-1-treated BAEC and with or without post-incubation with DMPO (100 μM). (B) Plot of the relative low-field EPR peak intensity of $Fe(MGD)_2$-NO. (C) eNOS activity as measured by conversion of arginine to citrulline from BAEC treated with SIN-1 with and without DMPO incubation. All data are means ± SEM, $^*P < 0.05$ versus control (untreated cells), $^{**}P < 0.05$ versus SIN-1-treated cells; one-way ANOVA, Tukey's test, $n = 3$.

SIN-1-mediated eNOS dysfunction is independent of BH_4 depletion

Treatment of BAEC with SIN-1 for 2 h in the absence of DMPO resulted in the depletion of BH_4 levels but upon incubation in plain media for additional 24 h, BH_4 levels were restored in SIN-1-challenged cells (Supporting Information Figure S6). This indicated that BH_4 was metabolically replenished after 24 h of incubation and that this occurred in the absence of DMPO. We also investigated the effect of DMPO on BH_4 levels in cells, within an hour of exposure to SIN-1 and found no change in the BH_4 levels, whiohc were similar to those in the absence of DMPO.

Dual roles of eNOS as target for both SIN-1 and DMPO

HEK293 cells were transfected with the cDNAs encoding both wild-type and mutant (S1179A) bovine eNOS. This mutant eNOS is resistant to phosphorylation and also does not exhibit any Akt-dependent increase in NO generation (Fulton *et al.*, 1999). Our Western blot results show equal transfection efficiency for both wild-type and mutant eNOS (Supporting Information Figure S7B) but no NO generation from mutant eNOS and with NO generation in wild-type eNOS-transfected cells were observed (Supporting Information Figure S7A). When HEK293 transfected cells were were treated with SIN-1 for 2 h, formation of O_2^- was observed, using DHE staining, in the cells transfected with wild-type eNOS-plasmid, whereas in mutant eNOS-transfected cells, $O_2^{\bullet-}$ generation was much lower (Figure 9A–C). EPR spin trapping to detect ROS generation in mutant eNOS-transfected cells gave low levels of ROS even after treatment with SIN-1 or DMPO (Figure 9D), confirming the important role of eNOS Ser^{1179} in generation of these free radicals. Phosphorylation of eNOS Ser^{1179} at low Ca^{2+} concentrations is known to be critical for O_2^- generation (Chen *et al.*, 2008).

To investigate whether DMPO could attenuate SIN-1-mediated ROS generation in HEK293 cells transfected with wild-type or mutant eNOS-plasmid, confocal microscopy with DCF-DA staining was used to detect ROS generation. We found that treatment with SIN-1 gave a ~4.4-fold increase in DCF-fluorescence intensity and was significantly reduced on post-treatment with DMPO (Supporting Information Figure S8A and B).

Discussion

Oxidative insult to eNOS can reverse its function from being an NO generator to a pro-oxidative enzyme, thereby exacerbating the degenerative processes that have been associated with endothelial dysfunction (Cai and Harrison, 2000). In these experiments, we have demonstrated how DMPO could reverse eNOS function from being pro-oxidative to that of its

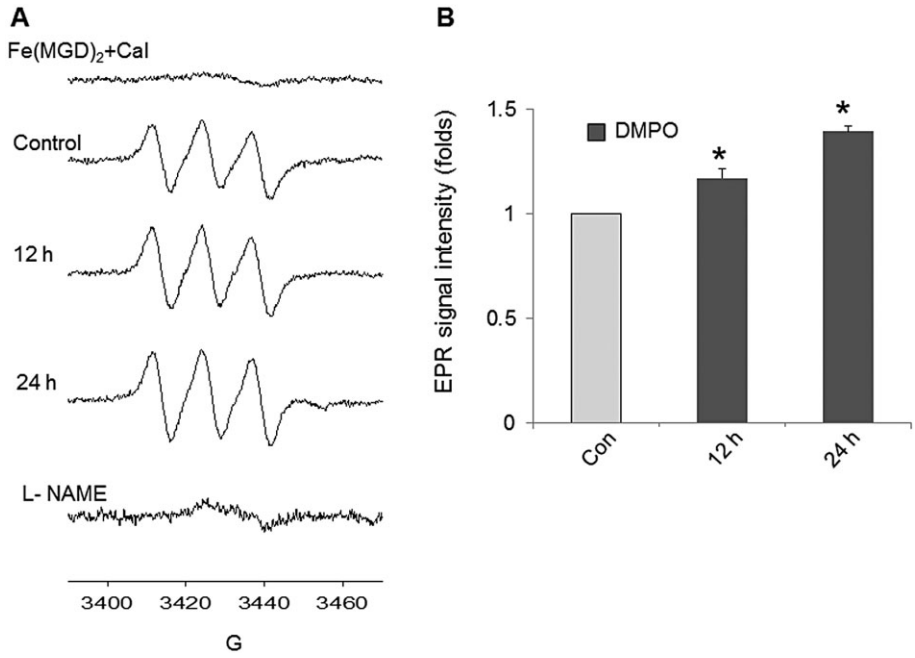

Figure 5

Time-dependent increase in NO production in DMPO-treated BAEC. (A) X-band EPR spectra of NO using $Fe(MGD)_2$ spin trap generated in BAEC during 0 to 24 h of incubation with DMPO (100 μM) and NOS inhibitor, L-NAME. (B) Plot of the relative low-field EPR peak intensity of $Fe(MGD)_2$-NO. Results are means ± SEM, $^*P < 0.05$ versus control (untreated cells); one-way ANOVA, Tukey's test, $n = 3$.

normal NO synthase function, by exploiting the ability of nitrones to regulate the nitroso-redox balance in the cell by scavenging ROS, increasing NO bioavailability and ultimately eNOS phosphorylation.

Post-treatment by DMPO of SIN-1-challenged BAEC conferred cytoprotection and restored NO production, while post-incubation of BAEC with SIN-1 for an additional 24 h in plain medium (in the absence of DMPO) gradually increased the oxidative burden on the cells. Production of $ONOO^-$ via formation of ROS and NO had been implicated in SIN-1 cytotoxicity to endothelial cells (Ishii *et al.*, 1999). Although nitrones are known to react with $ONOO^-$, where $ONOO^-$/ONOOH mediates the formation of the spin adducts using DMPO as spin trap (Gatti *et al.*, 1998; Nash *et al.*, 2012), the possibility that DMPO may be converting SIN-1 into a NO donor, rather than a $ONOO^-$ source, via $O_2^{\bullet-}$ scavenging is unlikely as 2 h of SIN-1 incubation with cells would not allow $ONOO^-$ to persist because of its short half-life (1.9 s at pH 7.4) (Beckman *et al.*, 1990) especially in a biological milieu. Furthermore, fluorescence studies showed that the half-time for the steady state $ONOO^-$ production from SIN-1 ranged from 14 to 26 min (Martin-Romero *et al.*, 2004). One could envision that after 2 h incubation of cells with SIN-1, $ONOO^-$ is released into the cell and could have had reacted, already causing oxidative damage, perhaps to eNOS. Therefore, the formation of ROS adducts we observed during spin trapping was not a direct reaction of $ONOO^-$ with DMPO. These results clearly suggested that post-treatment of cells with DMPO attenuated ROS production via eNOS dysfunction, in SIN-1-treated endothelial cells.

The ROS-derived $ONOO^-$ limits bioavailability of the eNOS cofactor, BH_4, resulting from either BH_4 depletion or oxidation and thus results in eNOS dysfunction (Kuzkaya *et al.*, 2003). Also, in BAEC, co-incubation of BH_4 or ascorbic acid with SIN-1 can reverse the effect of SIN-1 on NO production, perhaps via replenishment of oxidized BH_4 or reversal in the oxidation state of the redox-modified BH_4 (Xia *et al.*, 1998; Vasquez-Vivar *et al.*, 2002; Kuzkaya *et al.*, 2003). However, unlike ascorbic acid (Kuzkaya *et al.*, 2003), DMPO did not reverse eNOS function through restoration of BH_4 levels during initial and 24 h of SIN-1 treatments. So, the decrease in NO and increase in ROS we observed could have been the result of mechanisms, other than uncoupling of eNOS because of BH_4 depletion.

Therefore, the role of eNOS activation via phosphorylation was investigated to explain the observed increase in NO production in DMPO-treated cells. Phosphorylation of eNOS Ser^{1179} is known to activate eNOS by stimulating the flux of electrons within the reductase domain (McCabe *et al.*, 2000; Harris *et al.*, 2001; Michell *et al.*, 2001). Under oxidative stress conditions, eNOS generates $O_2^{\bullet-}$ and phosphorylation of eNOS Ser^{1179} is inhibited leading to decrease in NO production. How phosphorylation of eNOS Ser^{1179} is regulated to maintain the $O_2^{\bullet-}$-NO balance under oxidative stress conditions is not completely understood (Xia *et al.*, 1996) but it has been proposed that eNOS phosphorylation is redox-sensitive and is activated by the PI3K/Akt pathway (Dimmeler *et al.*, 1999; Fulton *et al.*, 1999) and by other kinases (Alhosin *et al.*, 2013). Regulation of ATP levels and activation of other kinases such as p38 MAPK and JNK by DMPO, therefore, warrants further investigation. This study, nevertheless,

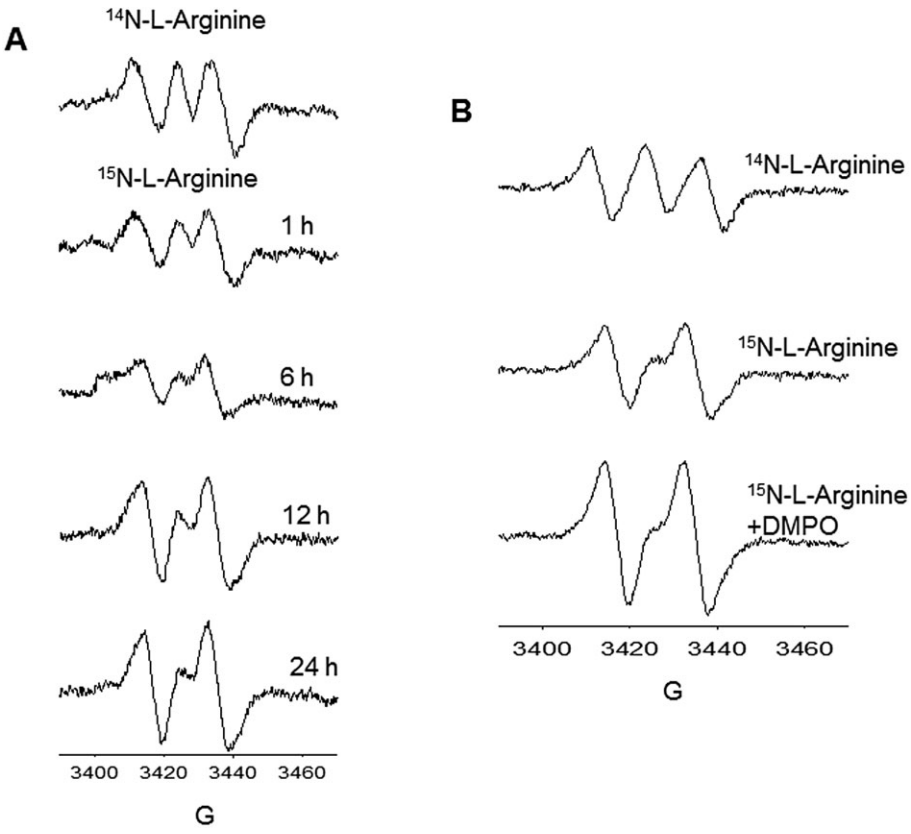

Figure 6

Determination of the source of NO. (A) X-band EPR spectra of ^{15}NO–Fe–MGD showing the characteristic doublet peak produced from BAEC supplemented with L-[^{15}N] arginine at various incubation times. (B) EPR spectra of NO adducts formed from BAEC incubated alone in medium containing L-[^{14}N] arginine; L-[^{15}N] arginine containing medium; and L-[^{15}N] arginine containing medium supplemented with DMPO. All experiments were performed at least three times.

demonstrates that DMPO could reverse eNOS dysfunction through decreased ROS production, increased NO bioavailability and increased phosphorylation of eNOS Ser^{1179} by activation of Akt.

Traditional antioxidants such as ascorbic acid and *N*-acetyl cysteine have been explored for their ability to prevent or reverse eNOS uncoupling in BAEC (Kuzkaya *et al.*, 2003) and in diabetic rat hearts (Okazaki *et al.*, 2011), through an increase in the BH_4/BH_2 ratio. Recently, lipophilic NO donor and lipophilic antioxidants, when introduced as a hybrid molecule and not as a mixture, exhibited protection from I/R injury in hearts, through significant reduction of infarct size with improved recovery of cardiac function (Rastaldo *et al.*, 2012). However, the mechanism of this protection was not clear. Moreover, magnesium lithospermate B protected endothelium from hyperglycaemia-induced dysfunction via eNOS phosphorylation, and induction of phase II enzymes by nuclear translocation of NRF-2, while α-lipoic acid did not cause these effects (Kim *et al.*, 2010).

Cardiometabolic disease is a growing health problem that derives from a combination of various risk factors such as hypertension, hyperglycaemia and elevated plasma triglyceride levels, leading to the development of type 2 diabetes and cardiovascular diseases. While the antioxidants mentioned above could be promising, their therapeutic application could be limited in the treatment of cardiometabolic diseases as unlike nitrones, their modes of action may only be limited to a few mechanisms (Zamora and Villamena, 2013). Findings presented in this present work and in our past studies (Durand *et al.*, 2009; Zuo *et al.*, 2009; Das *et al.*, 2012; Traynham *et al.*, 2012) showed that nitrones offered opportunities for their application in the treatment of cardiometabolic disorders such as hypertension and hyperglycaemia which are associated with endothelial dysfunction and depletion of cellular antioxidant pool. This is because as the nitrones not only scavenge ROS (Durand *et al.*, 2008; 2009) but also act through NO donation (Locigno *et al.*, 2005), by salvaging METC activity (Zuo *et al.*, 2009), by increasing METC biogenesis (Zuo *et al.*, 2009) by inhibiting mitochondrial polarization leading to down-regulation of proapoptotic signalling pathways, by inducing phase II enzyme activities via NRF-2 nuclear translocation (Das *et al.*, 2012), increasing myocyte contraction via increased sarcoplasmic reticulum Ca^{2+} handling (Traynham *et al.*, 2012) and, in this study, reversal of eNOS dysfunction.

Future work needs to investigate how DMPO activates Akt by immuno-spin trapping of the relevant proteins and role of nitrones as potential phosphatase inhibitors, as protein phosphatase 2A was also reported to decrease eNOS Ser^{1179} phosphorylation. Therefore, therapeutic agents that

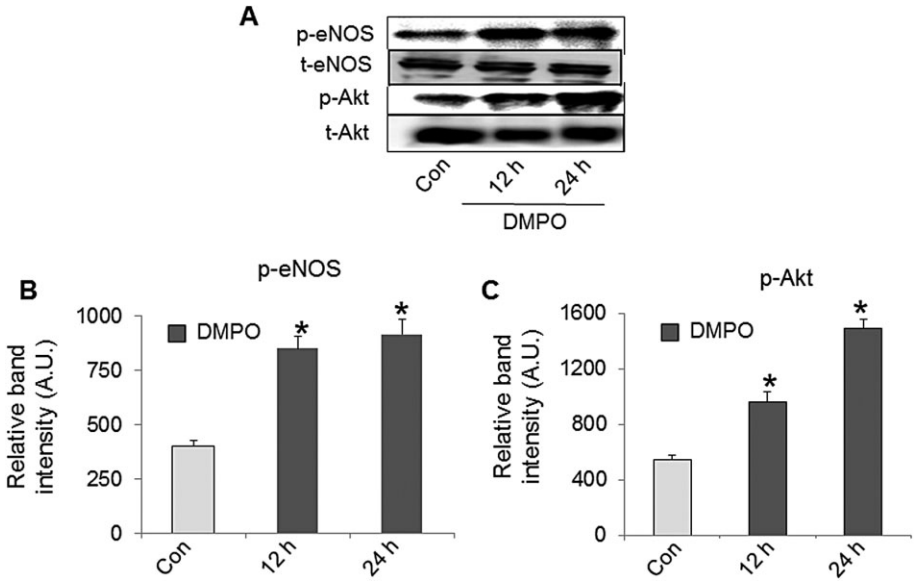

Figure 7

Effect of DMPO on the phosphorylation status of eNOS and AKT proteins in BAEC. (A) Western blot expression levels of p-eNOS, total eNOS, p-Akt and t-Akt in BAEC treated with 100 μM DMPO at 12 and 24 h incubation. Densitometric analysis of the expression levels of (B) p-eNOS (B) and (C) p-Akt. All data are means ± SEM, *$P < 0.05$ versus control (untreated cells), one-way ANOVA, Tukey's test, $n = 3$.

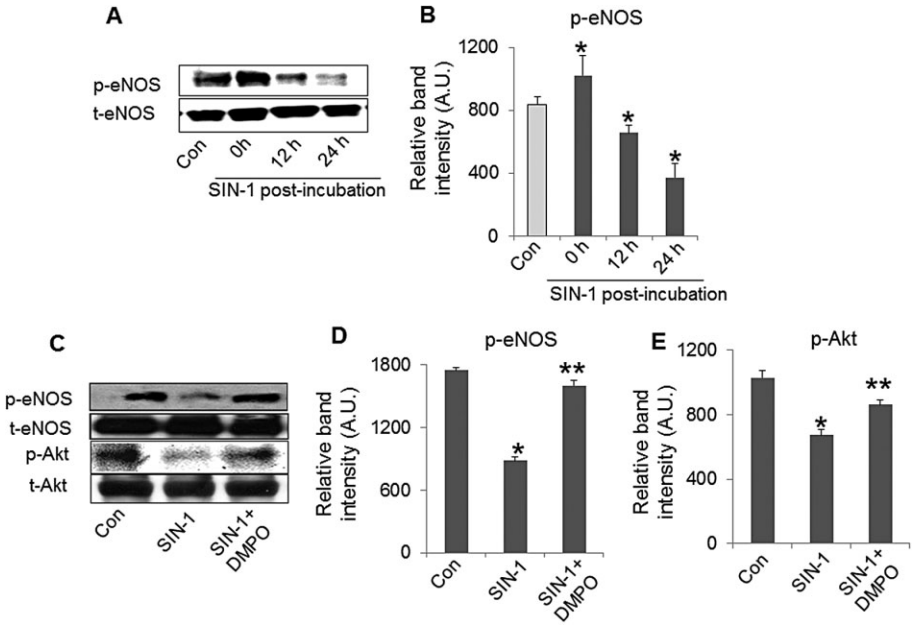

Figure 8

Modulation of eNOS and Akt phosphorylation by DMPO in SIN-1-treated cells. (A) Western blot analysis; and (B) densitometric analysis of p-eNOS Ser^{1179} and t-eNOS expression levels in BAEC treated with SIN-1 (500 μM, 2 h) and post-incubated in plain media (without SIN-1) at various incubation times. Results are represented as mean ± SEM,*$P < 0.05$ versus control (untreated cells). (C) Western blot analysis of p-eNOS Ser^{1179}, t-eNOS, p-Akt Ser^{473} and t-Akt expression in BAEC treated with SIN-1 (500 μM) alone and post-incubated with DMPO (100 μM). Densitometric analysis of the expression levels of (D) p-eNOS Ser^{1179} and (E) p-Akt from the above mentioned conditions. Results are represented as mean ± SEM, *$P < 0.05$ versus control (untreated cells), **$P < 0.05$ versus SIN-1-treated cells; one-way ANOVA, Tukey's test, $n = 3$.

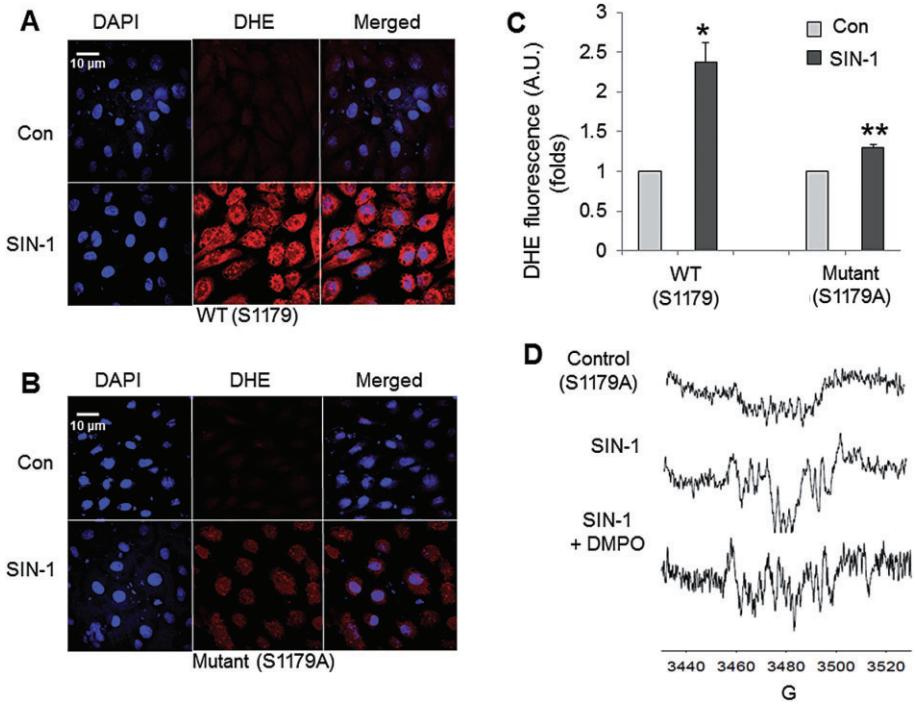

Figure 9

Detection of ROS generation in wild-type and mutant eNOS cDNA transfected HEK293 cells in the presence of SIN-1. Confocal DHE and DAPI images of untreated and SIN-1-treated HEK293 cells transfected with cDNAs encoding (A) wild-type eNOS Ser^{1179} (B) mutant eNOS cDNA S1179A. (C) Plot of relative average DHE-fluorescence intensities (n = 100 cells). Data are represented as mean ± SEM, *P < 0.05 versus control (non-transfected cells) and **P < 0.05 versus SIN-1-treated wild-type eNOS Ser^{1179} transfected cells; one-way ANOVA, Tukey's test, n=3. (D) X-band EPR detection of radical generation using EMPO/Me-β–CD from mutant eNOS cDNA transfected HEK293 cells that are untreated (top) and treated with SIN-1 (middle), and post-incubated with DMPO (bottom). All experiments were performed in triplicate.

can target the cytosolic matrix and affect kinase-mediated phosphorylation processes in the cell may be able to up-regulate eNOS. Attempts have been made to conjugate cyclic nitrones to several target-specific groups in order to facilitate their delivery to specific subcellular compartments (Durand *et al.*, 2003; 2009; 2010), as the poor target specificity of some of the natural antioxidants such as vitamin E, vitamin C, or lipoic acid limit their applications to the treatment of ROS-induced cardiovascular disorders (Willcox *et al.*, 2008; Shay *et al.*, 2009; Kizhakekuttu and Widlansky, 2010). Considering that eNOS is mostly localized near the cell membrane and that mitochondria and sarcoplasmic reticulum are mostly cytosolic, the use of nitrones that can specifically target these compartments would provide a way of identifying which targeted cellular event/s contributed the most to I/R injury and which target-specific nitrone will exhibit the most robust protection. Such studies would give valuable insights into the mechanisms of protection by nitrones. To date, targeting oxidative stress at the site/s of their origination still remains an attractive strategy for prevention and therapy of cardiovascular dysfunction (Munzel *et al.*, 2010). Therefore, a better understanding of the sources of free radicals and the mechanisms of oxidative stress, along with development of more target-specific antioxidants with multifunctional action, such as those exhibited by nitrones, are needed.

Acknowledgements

This work was funded by the NIH National Heart, Lung, and Blood Institute grant RO1 HL81248.

Conflict of interest

None.

References

Alexander SPH, Benson HE, Faccenda E, Pawson AJ, Sharman JL, Spedding M *et al.* (2013). The Concise Guide to PHARMACOLOGY 2013/14: Enzymes. Br J Pharmacol 170: 1797–1867.

Alhosin M, Anselm E, Rashid S, Kim JH, Madeira SV, Bronner C *et al.* (2013). Redox-sensitive up-regulation of eNOS by purple grape juice in endothelial cells: role of PI3-kinase/Akt, p38 MAPK, JNK, FoxO1 and FoxO3a. PLoS ONE 8: e57883.

Beckman JS, Beckman TW, Chen J, Marshall PA, Freeman BA (1990). Apparent hydroxyl radical production by peroxynitrite: implications for endothelial injury from nitric oxide and superoxide. Proc Natl Acad Sci U S A 87: 1620–1624.

Beckman JS, Koppenol WH (1996). Nitric oxide, superoxide, and peroxynitrite: the good, the bad, and ugly. Am J Physiol 271: 1424–1437.

Cai H, Harrison DG (2000). Endothelial dysfunction in cardiovascular diseases: the role of oxidant stress. Circ Res 87: 840–844.

Chen CA, Druhan LJ, Varadharaj S, Chen YR, Zweier JL (2008). Phosphorylation of endothelial nitric-oxide synthase regulates superoxide generation from the enzyme. J Biol Chem 283: 27038–27047.

Das A, Chakrabarty S, Choudhury D, Chakrabarti G (2010). 1,4-Benzoquinone (PBQ) induced toxicity in lung epithelial cells is mediated by the disruption of the microtubule network and activation of caspase-3. Chem Res Toxicol 23: 1054–1066.

Das A, Gopalakrishnan B, Voss OH, Doseff AI, Villamena FA (2012). Inhibition of ROS-induced apoptosis in endothelial cells by nitrone spin traps via induction of phase II enzymes and suppression of mitochondria-dependent pro-apoptotic signaling. Biochem Pharmacol 84: 486–497.

Dimmeler S, Fleming I, Fisslthaler B, Hermann C, Busse R, Zeiher AM (1999). Activation of nitric oxide synthase in endothelial cells by Akt-dependent phosphorylation. Nature 399: 601–605.

Dumitrescu C, Biondi R, Xia Y, Cardounel AJ, Druhan LJ, Ambrosio G *et al*. (2007). Myocardial ischemia results in tetrahydrobiopterin (BH4) oxidation with impaired endothelial function ameliorated by BH4. Proc Natl Acad Sci U S A 104: 15081–15086.

Durand G, Choteau F, Pucci B, Villamena FA (2008). Reactivity of superoxide radical anion and hydroperoxyl radical with alpha-phenyl-N-tert-butylnitrone (PBN) derivatives. J Phys Chem A 112: 12498–12509.

Durand G, Poeggeler B, Ortial S, Polidori A, Villamena FA, Boker J *et al*. (2010). Amphiphilic amide nitrones: a new class of protective agents acting as modifiers of mitochondrial metabolism. J Med Chem 53: 4849–4861.

Durand G, Polidori A, Salles JP, Pucci B (2003). Synthesis of a new family of glycolipidic nitrones as potential antioxidant drugs for neurodegenerative disorders. Bioorg Med Chem Lett 13: 859–862.

Durand G, Prosak RA, Han Y, Ortial S, Rockenbauer A, Pucci B *et al*. (2009). Spin trapping and cytoprotective properties of fluorinated amphiphilic carrier conjugates of cyclic versus linear nitrones. Chem Res Toxicol 22: 1570–1581.

Floyd RA (2009). Serendipitous findings while researching oxygen free radicals. Free Radic Biol Med 46: 1004–1013.

Floyd RA, Castro Faria Neto HC, Zimmerman GA, Hensley K, Towner RA (2013). Nitrone-based therapeutics for neurodegenerative diseases: Their use alone or in combination with lanthionines. Free Radic Biol Med 62: 145–156.

Floyd RA, Kopke RD, Choi CH, Foster SB, Doblas S, Towner RA (2008). Nitrones as therapeutics. Free Radic Biol Med 45: 1361–1374.

Forstermann U (2006). Janus-faced role of endothelial NO synthase in vascular disease: uncoupling of oxygen reduction from NO synthesis and its pharmacological reversal. Biol Chem 387: 1521–1533.

Fulton D, Gratton JP, McCabe TJ, Fontana J, Fujio Y, Walsh K *et al*. (1999). Regulation of endothelium-derived nitric oxide production by the protein kinase Akt. Nature 399: 597–601.

Gatti RM, Alvarez B, Vasquez-Vivar J, Radi R, Augusto O (1998). Formation of spin trap adducts during the decomposition of peroxynitrite. Arch Biochem Biophys 349: 36–46.

Giraldez RR, Zweier JL (1998). An improved assay for measurement of nitric oxide synthase activity in biological tissues. Anal Biochem 261: 29–35.

Gopalakrishnan B, Nash KM, Velayutham M, Villamena FA (2012). Detection of nitric oxide and superoxide radical anion by electron paramagnetic resonance spectroscopy from cells using spin traps. J Vis Exp 66: e2810.

Gross SS, Wolin MS (1995). Nitric oxide: pathophysiological mechanisms. Annu Rev Physiol 57: 737–769.

Harris MB, Ju H, Venema VJ, Liang H, Zou R, Michell BJ *et al*. (2001). Reciprocal phosphorylation and regulation of endothelial nitric-oxide synthase in response to bradykinin stimulation. J Biol Chem 276: 16587–16591.

Heitzer T, Schlinzig T, Krohn K, Meinertz T, Munzel T (2001). Endothelial dysfunction, oxidative stress, and risk of cardiovascular events in patients with coronary artery disease. Circulation 104: 2673–2678.

Hyland K (1985). Estimation of tetrahydro, dihydro and fully oxidised pterins by high-performance liquid chromatography using sequential electrochemical and fluorometric detection. J Chromatogr 343: 35–41.

Ishii M, Shimizu S, Momose K, Yamamoto T (1999). SIN-1-induced cytotoxicity in cultured endothelial cells involves reactive oxygen species and nitric oxide: protective effect of sepiapterin. J Cardiovasc Pharmacol 33: 295–300.

Kim SH, Kim SH, Choi M, Lee Y, Kim YO, Ahn DS *et al*. (2010). Natural therapeutic magnesium lithospermate B potently protects the endothelium from hyperglycaemia-induced dysfunction. Cardiovasc Res 87: 713–722.

Kizhakekuttu TJ, Widlansky ME (2010). Natural antioxidants and hypertension: promise and challenges. Cardiovasc Ther 28: e20–e32.

Kuzkaya N, Weissmann N, Harrison DG, Dikalov S (2003). Interactions of peroxynitrite, tetrahydrobiopterin, ascorbic acid, and thiols: implications for uncoupling endothelial nitric-oxide synthase. J Biol Chem 278: 22546–22554.

Lin MI, Fulton D, Babbitt R, Fleming I, Busse R, Pritchard KA Jr *et al*. (2003). Phosphorylation of threonine 497 in endothelial nitric-oxide synthase coordinates the coupling of L-arginine metabolism to efficient nitric oxide production. J Biol Chem 278: 44719–44726.

Locigno EJ, Zweier JL, Villamena FA (2005). Nitric oxide release from the unimolecular decomposition of the superoxide radical anion adduct of cyclic nitrones in aqueous medium. Org Biomol Chem 3: 3220–3227.

Lomonosova EE, Kirsch M, Rauen U, de Groot H (1998). The critical role of Hepes in SIN-1 cytotoxicity, peroxynitrite versus hydrogen peroxide. Free Radic Biol Med 24: 522–528.

McCabe TJ, Fulton D, Roman LJ, Sessa WC (2000). Enhanced electron flux and reduced calmodulin dissociation may explain 'calcium-independent' eNOS activation by phosphorylation. J Biol Chem 275: 6123–6128.

Martin-Romero FJ, Gutierrez-Martin Y, Henao F, Gutierrez-Merino C (2004). Fluorescence measurements of steady state peroxynitrite production upon SIN-1 decomposition: NADH versus dihydrodichlorofluorescein and dihydrorhodamine 123. J Fluoresc 14: 17–23.

Michell BJ, Chen ZP, Tiganis T, Stapleton D, Katsis F, Power DA *et al*. (2001). Coordinated control of endothelial nitric-oxide

synthase phosphorylation by protein kinase C and the cAMP-dependent protein kinase. J Biol Chem 276: 17625–17628.

Munzel T, Gori T, Bruno RM, Taddei S (2010). Is oxidative stress a therapeutic target in cardiovascular disease? Eur Heart J 31: 2741–2748.

Nash KM, Rockenbauer A, Villamena FA (2012). Reactive nitrogen species reactivities with nitrones: theoretical and experimental studies. Chem Res Toxicol 25: 1581–1597.

O'Donnell VB, Freeman BA (2001). Interactions between nitric oxide and lipid oxidation pathways: implications for vascular disease. Circ Res 88: 12–21.

Okazaki T, Otani H, Shimazu T, Yoshioka K, Fujita M, Iwasaka T (2011). Ascorbic acid and N-acetyl cysteine prevent uncoupling of nitric oxide synthase and increase tolerance to ischemia/reperfusion injury in diabetic rat heart. Free Radic Res 45: 1173–1183.

Rastaldo R, Cappello S, Di Stilo A, Folino A, Losano G, Pagliaro P (2012). A lipophilic nitric oxide donor and a lipophilic antioxidant compound protect rat heart against ischemia-reperfusion injury if given as hybrid molecule but not as a mixture. J Cardiovasc Pharmacol 59: 241–248.

Rockenbauer A, Korecz L (1996). Automatic computer simulations of ESR spectra. Appl Magn Reson 10: 29–43.

Shay KP, Moreau RF, Smith EJ, Smith AR, Hagen TM (2009). Alpha-lipoic acid as a dietary supplement: molecular mechanisms and therapeutic potential. Biochim Biophys Acta 1790: 1149–1160.

Shinobu LA, Jones SG, Jones MM (1984). Sodium N-methyl-D-glucamine dithiocarbamate and cadmium intoxication. Acta Pharmacol Toxicol (Copenh) 54: 189–194.

Šnyrychová I (2010). Improvement of the sensitivity of EPR spin trapping in biological systems by cyclodextrins: a model study with thylakoids and photosystem II particles. Free Radic Biol Med 48: 264–274.

Tosaki A, Blasig IE, Pali T, Ebert B (1990). Heart protection and radical trapping by DMPO during reperfusion in isolated working rat hearts. Free Radic Biol Med 8: 363–372.

Traynham CJ, Roof SR, Wang H, Prosak RA, Tang L, Viatchenko-Karpinski S *et al*. (2012). Diesterified nitrone rescues nitroso-redox levels and increases myocyte contraction via increased SR Ca2+ handling. PLoS ONE 7: e52005.

Vasquez-Vivar J, Martasek P, Whitsett J, Joseph J, Kalyanaraman B (2002). The ratio between tetrahydrobiopterin and oxidized tetrahydrobiopterin analogues controls superoxide release from endothelial nitric oxide synthase: an EPR spin trapping study. Biochem J 362: 733–739.

Villamena FA, Das A, Nash KM (2012). Potential implication of the chemical properties and bioactivity of nitrone spin traps for therapeutics. Future Med Chem 4: 1171–1207.

Villamena FA, Hadad CM, Zweier JL (2005). Comparative DFT study of the spin trapping of methyl, mercapto, hydroperoxy, superoxide, and nitric oxide radicals by various substituted cyclic nitrones. J Phys Chem A 109: 1662–1674.

Villamena FA, Zweier JL (2004). Detection of reactive oxygen and nitrogen species by EPR spin trapping. Antioxid Redox Signal 6: 619–629.

Vita JA (2011). Endothelial function. Circulation 124: e906–e912.

Wang PG, Cai TB, Taniguchi N (2005). Nitric Oxide Donors. Wiley-VCH Verlag GmbH & Co: Weinheim.

Wei CC, Crane BR, Stuehr DJ (2003). Tetrahydrobiopterin radical enzymology. Chem Rev 103: 2365–2383.

Willcox BJ, Curb JD, Rodriguez BL (2008). Antioxidants in cardiovascular health and disease: key lessons from epidemiologic studies. Am J Cardiol 101: 75D–86D.

Xia Y, Dawson VL, Dawson TM, Snyder SH, Zweier JL (1996). Nitric oxide synthase generates superoxide and nitric oxide in arginine-depleted cells leading to peroxynitrite-mediated cellular injury. Proc Natl Acad Sci U S A 93: 6770–6774.

Xia Y, Tsai AL, Berka V, Zweier JL (1998). Superoxide generation from endothelial nitric-oxide synthase. A Ca2+/.calmodulin-dependent and tetrahydrobiopterin regulatory process. J Biol Chem 273: 25804–25808.

Xia Y, Zweier JL (1997). Direct measurement of nitric oxide generation from nitric oxide synthase. Proc Natl Acad Sci U S A 94: 12705–12710.

Zamora PL, Villamena FA (2013). Pharmacological approaches to the treatment of oxidative stress-induced cardiovascular dysfunctions. Future Med Chem 5: 465–478.

Zuo L, Chen YR, Reyes LA, Lee HL, Chen CL, Villamena FA *et al*. (2009). The radical trap 5,5-dimethyl-1-pyrroline N-oxide exerts dose-dependent protection against myocardial ischemia-reperfusion injury through preservation of mitochondrial electron transport. J Pharmacol Exp Ther 329: 515–523.

Supporting information

Additional Supporting Information may be found in the online version of this article at the publisher's web-site:

http://dx.doi.org/10.1111/bph.12572

Figure S1 Cytotoxicity of DMPO alone on BAEC. BAEC viability after incubation with DMPO (0–500 μM) as determined by MTT assay. Data are represented as the mean ± SEM, $n = 6$.

Figure S2 Time-dependent cytotoxicity of SIN-1 on BAEC. Time-dependent cytotoxic effects of SIN-1 (500 μM) on BAEC as determined by MTT assay at various time points (A) 1–6 h. BAEC were treated with SIN-1 for 2 h and post-incubated with plain media (without SIN-1) at various time points (B) 0–24 h. Cell viability was assessed by MTT assay. Data are represented as the mean ± SEM, $^*P < 0.05$ versus control (untreated cells), $n = 6$.

Figure S3 Detection of O_2^- generation in SIN-1-treated BAEC by EPR. (A) BAEC were treated with SIN-1 for 2 h and post-incubated in plain media (without SIN-1) at various time points (0–24 h), and ROS generation was monitored by X-band EPR spectrometer using EMPO and Me-β–CD as the spin traps. (B) A plot of relative ROS intensities for the untreated and SIN-1-treated BAEC, post-incubated in plain media at various time points (0–24 h). Data are represented as mean ± SEM, $^*P < 0.05$ versus control (untreated cells), $n = 3$.

Figure S4 Detection of $O_2^{\bullet-}$ generation in SIN-1-treated BAEC by fluorescence. (A) $O_2^{\bullet-}$ generation in untreated BAEC, and cells treated with SIN-1 (500 μM) and post-incubated with plain media at various points were monitored by confocal microscopy using DHE. The figure represents the merged image of DHE-fluorescence (red) and DAPI-fluorescence (blue), bar represents 10 microns. (B) A plot of

relative DHE-fluorescence obtained from the average of 100 cells. Data are represented as mean ± SEM, *P < 0.05 versus control (untreated cells).

Figure S5 Detection of ROS generation in SIN-1-treated BAEC by fluorescence. (A) Generation of ROS in untreated BAEC, and cells treated with SIN-1 (500 μM) and post-incubated with plain media at various time points were monitored by confocal microscopy using ROS-specific fluorescence dye CM-H_2DCFDA. The figure represents the merged image of DCF-fluorescence (green) and DAPI-fluorescence (blue), bar represents 10 microns. (B) A plot of relative DCF-fluorescence obtained from the average of 100 cells. Data are represented as mean ± SEM, *P < 0.05 (vs.) control (untreated cells).

Figure S6 Determination of BH_4 depletion by SIN-1-mediated eNOS dysfunction. The levels of BH_4 in SIN-1-treated BAEC alone and post-incubated with DMPO was measured to determine the extent of eNOS uncoupling. (A) The BH_4 chromatograms obtained at retention time of ~18 min. BAEC treated with SIN-1-post-incubated for 0 h and 24 h. (B) Respective BH_4 chromatograms for BAEC alone, treated with SIN-1, and post-incubated with DMPO for 2 h. All experiments were performed at least three times.

Figure S7 Detection of NO in non-transfected and transfected HEK293 cells. (A) NO generation in non-transfected and wild-type/mutant eNOS cDNA transfected HEK293 cells was monitored by X-band EPR spectrometer using $Fe(MGD)_2$ as a spin trap upon stimulation with CaI. From top to bottom: Spectrum 1 represents NO generated from non-transfected HEK293 cells as control; Spectrum 2 represents NO generated from HEK293 cells transfected with wild-type eNOS cDNA (Ser-1779); Spectrum 3 represents NO generated from HEK293 cells transfected with mutant eNOS cDNA (Ser-1779A); and Spectrum 4 represents NO generated from HEK293 cells transfected with wild-type eNOS cDNA (Ser-1779) and treated with the NOS inhibitor L-NAME. (B) Representative Western blot expression levels of eNOS protein from HEK293 cells transfected with cDNAs encoding wild-type eNOS S1179 and mutant eNOS cDNA S1179A and the corresponding loading control (β-actin). (C) A plot of relative NO intensities from non-transfected and transfected HEK cells. Data are represented as mean ± SEM, *P < 0.05 versus control (untreated non- transfected cells), **P < 0.05 versus WT eNOS treated cells, n = 3.

Figure S8 Attenuation of SIN-1-mediated ROS generation in wild-type eNOS-plasmid transfected HEK293 cells by DMPO. (A) Confocal micrographs using DCF-DA for ROS detection of wild-type eNOS-cDNA transfected HEK293 cells treated with SIN-1 (500 μM) alone and with post-incubation with nitrone DMPO (100 μM). White bar corresponds to 10 microns. (B) Plot of relative DCF-fluorescence obtained from an average of 100 cells. Data are represented as mean ± SEM, *P < 0.05 versus control, **P < 0.05 versus SIN-1-treated cells, n = 3.

Table S1 Simulated EPR parameters and concentrations of various adducts formed from SIN-1 treatment of BEAC alone as a function of time obtained by EPR spin trapping using EMPO/methylated-β-cyclodextrin as spin traps.

Table S2 Simulated EPR parameters and concentrations of various adducts formed from post-incubation with DMPO of SIN-1-treated BAEC obtained by EPR spin trapping using EMPO/methylated-β-cyclodextrin as spin traps.

Table S3 Simulated EPR parameters various adducts formed from EMPO/methylated-β-cyclodextrin as spin traps using independently generated HOO, HO and C-centred radicals from hypoxanthine-xanthine oxidase, H_2O_2-Fe^{2+} and H_2O_2-Fe^{2+}-EtOH systems.